JOURNAL OF SYNCHROTRON RADIATION

Volume 28 (2021)

Supporting information for article:

The fast multi-frame X-ray diffraction detector at the Dynamic Compression Sector

N. W. Sinclair, S. J. Turneaure, Y. Wang, K. Zimmerman and Y. M. Gupta

DQE Measurement

This is a more in-depth discussion of the DQE measurement presented in the article.

Before measuring the DQE, the four-frame detector was calibrated to determine the total conversion gain, relating the number of input photons to counts on the detector. The detector was configured with the 75:40 mm fiber taper, the external image intensifier at maximum gain (specified at 4000 W_{out}/W_{in}), and one of our most sensitive X-ray phosphor plates (having an areal density of 81 mg/cm^2). The x-ray beam was attenuated with 6.5 mm of aluminum and scattered by a 4 mm-thick piece of glassy carbon located 168 cm from the detector. A Pb mask blocked all but a small detector region of interest (ROI), allowing the photon flux beyond the mask to be measured by a calibrated PIN diode before taking images with the detector. X-ray exposures with a 20 microsecond duration were captured with the detector, averaging many full storage ring cycles. A single 23 keV X-ray photon striking the detector produced 4300 counts on one of the ICCD cameras.

With this calibration, the DQE can be measured as the ratio of the squared, measured SNR, to the squared, ideal SNR, assuming Poisson statistics of the incoming photons. As stated in the article, fifty repeated images of this masked region were taken with a mean of 3300 X-ray photons and a standard deviation of 106 photons. This noise level would suggest a DQE of 0.29 if the incident photons followed Poisson statistics with a fixed mean photon number.

There is a significant contribution to this variation from temporal variation of the incident beam intensity. Removing the Pb mask and observing the fluctuation of multiple ROIs with a wide range of signal levels, the same process to quantify DQE yields dramatically different values depending on the level of illumination, with the DQE trending toward zero at very high photon numbers. Figure 1(a) shows the measured DQE in several ROIs with varying levels of illumination (along with model curves, explained below) from 20 repeated images, demonstrating the apparent degradation of the DQE with increasing signal level, as the measured SNRs approach a constant value, while the SNR of an ideal detector would continue improving with signal level. The ROIs were chosen to be large compared to the point-spread function of the detector, so that the DQE is not artificially inflated, as described in Gruner et al (1993). Beam intensity fluctuations with a standard deviation of only 2% are needed to explain this variation, which is conceivable with this beam configuration due to fluctuations in pointing from the upstream Kirkpatrick-Baez (K-B) mirrors and associated changes in attenuation from the filters or scattering from the source.

Moving forward under the assumption that the reduction in DQE with signal level is due to fluctuations in the input beam, we can attempt to include these fluctuations in a model and extract an approximate measure of the DQE without these fluctuations. We assume an initial Poisson distribution of N_0 photons and a binomial process of attenuation and scattering, with a probability, p, of each photon being transmitted to the detector ROI, so that the mean number of photons reaching the phosphor, N_i, is pN_0. If we allow the transmission probability, p, to fluctuate, then the variance in the number of incident photons is given by the law of total variance:

$$\sigma_i^2 = Var(N_i) = E[Var(\hat{N}_i|\hat{p})] + Var(E[\hat{N}_i|\hat{p}]) = E[\hat{N}_0\hat{p}(1-\hat{p})] + Var(\hat{p}\hat{N}_0)$$
$$\sigma_i^2 = N_0 p(1-p) + \sigma_{N_0}^2\sigma_p^2 + p^2\sigma_{N_0}^2 + N_0^2\sigma_p^2 \qquad \text{(Eqn.1)}$$
$$\sigma_i^2 = N_i\left(1 + \left(\frac{\sigma_p}{p}\right)^2 (N_i + p)\right),$$

where σ_p^2 denotes the variance in the transmission probability.

Vartsky et al. (2009) demonstrate how the noise introduced in each stage of signal conversion in a detector determines the variance of the total signal and provide an equation for calculating the DQE. Following that method, we could characterize our system by several stages of conversion, subsequent to this loss process, e.g. conversion to visible light, gain in the first image intensifier, etc., and we could use the equation introduced in Vartsky et al. (2009) to estimate the DQE, as follows:

$$DQE = \frac{QE}{1 + \sum_k \left(\frac{\sigma_k}{\mu_k}\right)^2 \frac{1}{\prod_{n=1..k-1} \mu_n}} \qquad \text{(Eqn.2)}$$

where k denotes a stage of amplification. This equation has been restructured somewhat from its previous publication, where the numbering of stages is now from first stage to last, and the QE of the phosphor has been included, since this was not considered in their proton detector. While this can produce an estimate of the DQE, observing the form allows a slight modification to predict the apparent DQE observed from a detector with a noisy input (also explicitly derived in the following section). The one in the denominator represents the variance due to the Poisson statistics of the input, and replacing that variance by the variance found in Eqn. 1, gives the apparent DQE with increased input fluctuations, specifically:

$$DQE = \frac{QE}{1 + \left(\frac{\sigma_p}{p}\right)^2 (N_i + p) + \alpha}, \qquad \text{(Eqn.3)}$$

where the sum over the contributions from each detector stage have been absorbed into α. The dependence of the apparent DQE on incident N_i has been plotted in Figure 1a, for varying values of α, along with the measured DQE values from the detector data. For the plotted apparent DQE curves, the factor $\frac{\sigma_p}{p}$ was taken to be 0.02, measured by the ratio of standard deviation to mean signal at very high photon numbers, in this case by looking at the variation of the entire frame ($N_i = 3\text{x}10^6$). These lines are labeled with a DQE value, corresponding to the DQE value the detector would display with no input noise beyond Poisson statistics. The highest value of DQE plotted is 90%, as this roughly corresponds to the maximum DQE possible with a phosphor QE of 0.92. Clearly, there is far too much scatter in the data to determine a precise DQE, but the data suggests the DQE is unlikely to be lower than 30%.

Figure 1b shows the same DQE measurements along with simulated DQE measurements from a detector with a DQE of 0.42 and 20 repeated frames N, to demonstrate the pattern of scatter in the results in comparison to a line plotting Eqn. 3 for this DQE. For each data point

in the simulation, a mean incident photon number, λ, is drawn from a normal distribution (with $\frac{\sigma_p}{p}$=0.02, to represent the excess input beam fluctuations) and a Poisson distribution of photons, with mean λ, is sampled to determine the incident x-ray number, N_{inc}. Subsequently, a normal distribution was sampled QE*N_{inc} times to determine a total signal from the detector, where this normal distribution is a stand-in for the entire cascade conversion process from x-ray to signal on the ICCD. The standard deviation of this normal distribution was chosen to produce the desired DQE level (i.e. 0.42) using Eqn. 3. The modeled data demonstrates the strongly asymmetric scatter in the data, showing a tendency to produce very large DQE measurements at low photon number, similar to the wide spread of real measurement in that region. The DQE level of 0.42 was chosen somewhat arbitrarily, as the cloud of simulated measurements has acceptable overlap with the measured data between 40 and 60%, suggesting this range is a reasonable estimate of the detector DQE. Similar plots of the data alongside simulations with a DQE of 0.3, 0.5, and 0.6 are displayed in Figure 2.

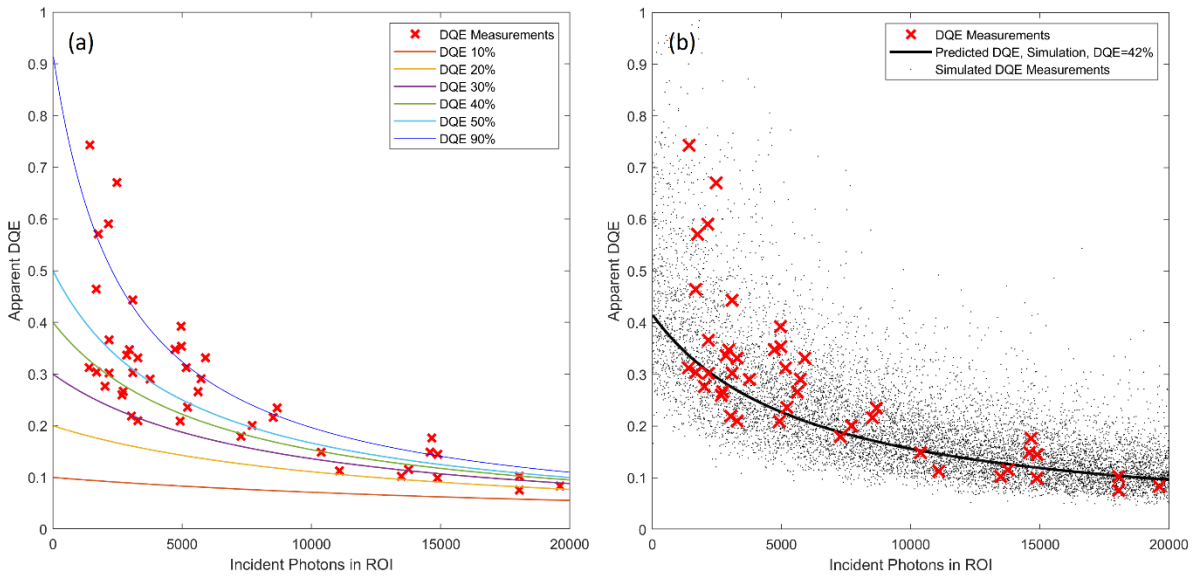

Figure 1 DQE Simulations and Measurements. (a) Measurements of DQE, inferred from the measured signal-to-noise ratio, with varying photon number in the ROI, along with lines showing the expected DQE with a fluctuating number of input photons, as defined by Eqn. 3 with $\frac{\sigma_p}{p}$*= 0.02. (b) The same DQE measurements are plotted alongside simulated DQE measurements, assuming a DQE of 0.42 and* $\frac{\sigma_p}{p}$ *=0.02, demonstrating the pattern of the scattered data points.*

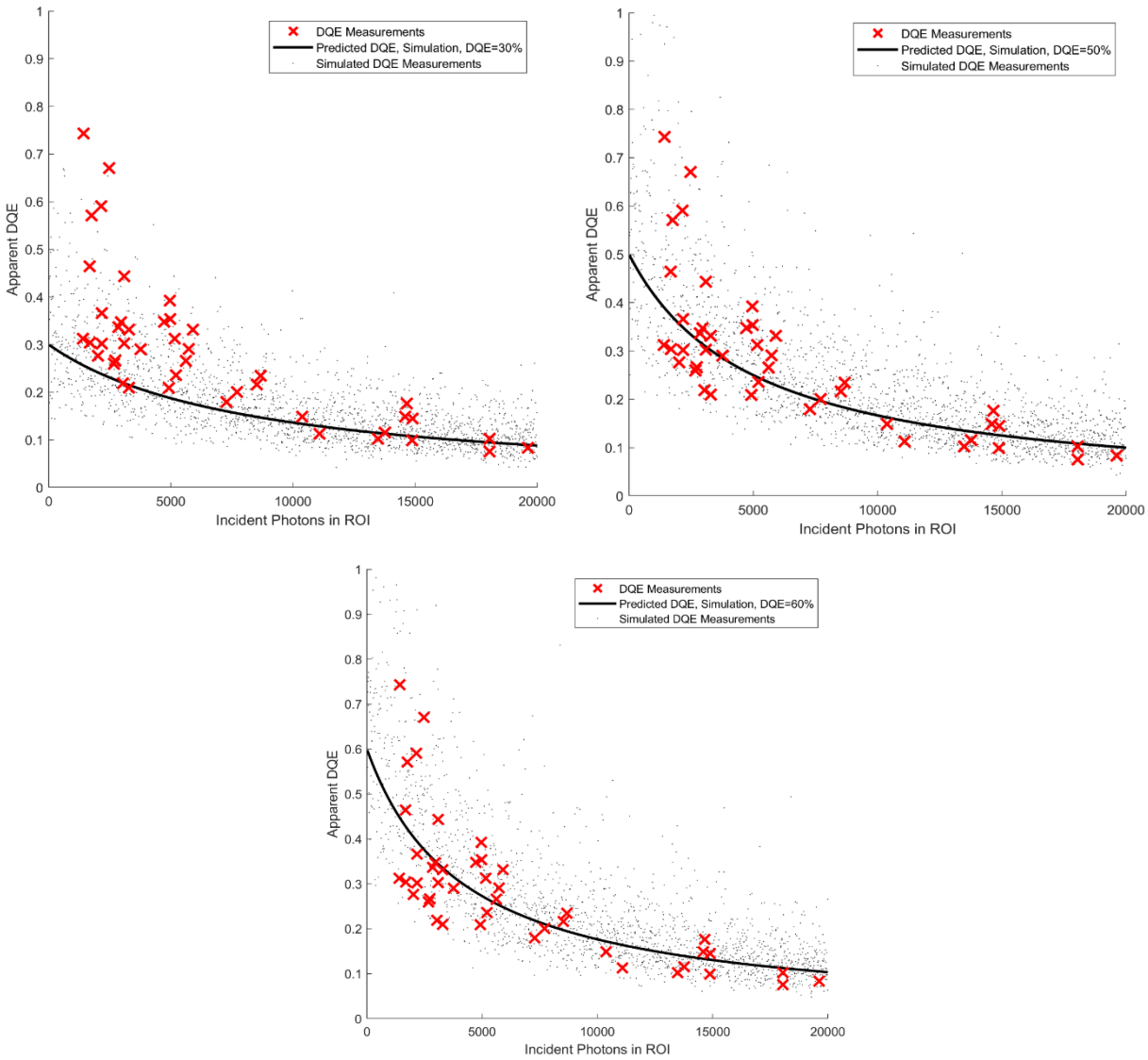

Figure 2 Comparisons of Measured DQE Data Points to Simulations with Varying DQE, with DQE = 0.3, 0.4, and 0.6, to contrast with the plot of DQE = 0.42 in Figure 1.

Noise Model, DQE Estimate Calculation Overview

The system can be broken down into absorption and 3 subsequent conversion stages, and for each stage, a μ_k and σ_k will be defined for use in Eqn. 3. These stages are 1) conversion to visible light and propagation to the image intensifier, 2) image intensifier gain and propagation to the ICCDs, and 3) ICCD gain and conversion to an electronic signal. Here, each stage will be briefly explained, noting the appropriate parameters, μ_k and σ_k. The parameters are explained in more detail in the following section, examining each stage individually.

The first stage is the phosphor conversion to visible light, combined with the subsequent losses before the light reaches the first image intensifier. The mean gain, μ_1, is determined by the LSO:Ce light yield, approximately 23000 photons/keV for 23.5 keV x-rays (Wanarak et al., 2012), as well as the loss in the phosphor, loss in fiber coupling, and loss in the fiber taper. The losses are not well-characterized, but, since the gains of the rest of the stages are predictable, the total conversion gain (4300 counts/photon) divided by the other stage gains provides a rough estimate of this loss (yielding a factor of 0.0082 for transmission to the intensifier). The noise from this process, or more specifically $\frac{\sigma_1}{\mu_1}$, can be determined from the intrinsic resolution of the LSO:Ce (FWHM $\frac{\Delta E}{E}$ = ~40% (Syntfeld-Kazuch, 2009; Wanarak (2012), yielding $\frac{\sigma_1}{\mu_1}$ = 0.17.

The image intensifier on the front-end of the system introduces a large amount of noise to the system, in particular due to its poor photocathode sensitivity for the LSO:Ce emission (QE=0.13 for 420 nm light). For the gain of the intensifier, the manufacturer's measured gain is 4000 photons out per incident photon. Unfortunately, the noise factor for this image intensifier has not been directly measured. Vartsky et al. (2009) used a similar image intensifier, quantifying the pulse height distribution of the output, which suggests a reasonable range for $\frac{\sigma_2}{\mu_2}$ is 3 to 4. For context, with no noise from the amplification, the QE alone would yield $\frac{\sigma_2}{\mu_2}$ =2.6. Following the intensifier output, the signal is decreased by losses due to demagnifying lens coupling and by a factor of four by the beamsplitters. From lens coupling, with a magnification of 0.625 and a f-number of 2, the signal is reduced by a factor of 0.00925, using the equation given in Gruner et al. (2002). Taken together, the intensifier gain, optical losses, and beamsplitting yield μ_2 = 9.25.

The ICCD photocathode has much better QE than that of the front-end image intensifier, with QE=0.35 at 420 nm. Similar to the front-end image intensifier, we don't have a direct measurement of the noise performance of this camera, but we can make an estimate by assuming that the noise characteristics of its internal intensifier's MCP are similar to that of the front-end image intensifier. Using the same range of MCP noise that yielded an estimate of $\frac{\sigma_2}{\mu_2}$ = 3 to 4, with a QE of 0.35, yields $\frac{\sigma_3}{\mu_3}$ = 1.6 to 2.3.

Taken altogether, using Eqn. 3 these parameter ranges yield an expected DQE for the entire system of between 0.30 and 0.19.

DQE Estimate Calculation, Details of Each Stage and Final Calculation

This section contains the derivation of the variance at each stage as well as a discussion of the parameter values that characterize each stage. At the end of this section, the estimated DQE is calculated from these parameters.

Beam Intensity Fluctuations

We will write down the variance of the signal in two model cases, one with photons arriving at the phosphor with a Poisson distribution and one simulating a fluctuating beam intensity, with photons arriving at the phosphor after going through a binomial loss process with the mean varying between trials. The first case will represent the model that we will use to estimate DQE (as described in the previous section), and the second will give an expression for the DQE that one would measure with a fluctuating input (the source of Eqn. 3).

- Below 'E[]' stands for expectation value, 'Var()' and 'σ^2' are both used to note variance.
- N_0: Initial flux of photons before absorption/scattering.

After binomial loss from attenuator absorption and scattering, mean photon count goes to $N_{inc} = N_0 p$, where p is the probability of transmission of a single photon to the phosphor.

$$\sigma_{\mathrm{inc}}^2 = \mathrm{E}\left[\mathrm{Var}\left(\mathrm{N_{inc}}\middle|\widehat{\mathrm{N_0}},\hat{\mathrm{p}}\right)\right] + \mathrm{Var}\left(\mathrm{E}\left[\mathrm{N_{inc}}\middle|\widehat{\mathrm{N_0}},\hat{\mathrm{p}}\right]\right) = \overline{\mathrm{N}}_0\overline{\mathrm{p}}(1-\overline{\mathrm{p}}) + \mathrm{Var}\left(\widehat{\mathrm{N_0}}\hat{\mathrm{p}}\right)$$

$$\sigma_{\mathrm{inc}}^2 = \overline{\mathrm{N}}_0\overline{\mathrm{p}}(1-\overline{\mathrm{p}}) + \sigma_{\mathrm{N0}}^2\sigma_{\mathrm{p}}^2 + \sigma_{\mathrm{N0}}^2\overline{\mathrm{p}}^2 + \overline{\mathrm{N}}_0^2\sigma_{\mathrm{p}}^2 = \overline{\mathrm{N}}_0\overline{\mathrm{p}} + \overline{\mathrm{N}}_0\sigma_{\mathrm{p}}^2 + \overline{\mathrm{N}}_0^2\sigma_{\mathrm{p}}^2$$

$$\sigma_{\mathrm{inc}}^2 = \overline{\mathrm{N}}_0\overline{\mathrm{p}}\left(1+\frac{\sigma_{\mathrm{p}}^2}{\overline{\mathrm{p}}^2}\left(\overline{\mathrm{N}}_0\overline{\mathrm{p}}+\overline{\mathrm{p}}\right)\right) = \overline{\mathrm{N}}_{\mathrm{inc}}\left(1+\frac{\sigma_{\mathrm{p}}^2}{\mathrm{p}^2}\left(\overline{\mathrm{N}}_{\mathrm{inc}}+\overline{\mathrm{p}}\right)\right))$$

In the first case, $\sigma_{\mathrm{p}}^2 = 0$, and this reduces back to Poisson statistics. In the case of fluctuating absorption, we retain this excess variation to propagate to future stages. The mean transmission, p, is very small compared with the $\overline{\mathrm{N}}_{\mathrm{inc}}$, so the contribution of the final term is essentially negligible.

Absorption: Phosphor screen absorption

QE given by η

Expression for Variance:

Random variable N_{abs} with $\mu_{abs} = \eta N_{inc}$

$$\sigma_{\mathrm{abs}}^2 = \mathrm{E}\left[\mathrm{Var}\left(\mathrm{N_{abs}}\middle|\widehat{\mathrm{N}}_{\mathrm{inc}}\right)\right] + \mathrm{Var}(\mathrm{E}[\mathrm{N_{abs}}|\mathrm{N_{inc}}]) = \overline{\mathrm{N}}_{\mathrm{inc}}\eta(1-\eta) + \mathrm{Var}\left(\eta\widehat{\mathrm{N}_{\mathrm{inc}}}\right)$$

$$\sigma_{\mathrm{abs}}^2 = \overline{\mathrm{N}}_{\mathrm{inc}}\eta(1-\eta) + \eta^2\ \mathrm{Var}\left(\widehat{\mathrm{N}_{\mathrm{inc}}}\right) = \overline{\mathrm{N}}_{\mathrm{inc}}\eta(1-\eta) + \eta^2\overline{\mathrm{N}}_{\mathrm{inc}}\left(1+\frac{\sigma_{\mathrm{p}}^2}{\mathrm{p}^2}\left(\overline{\mathrm{N}}_{\mathrm{inc}}+\overline{\mathrm{p}}\right)\right))$$

$$\sigma_{\mathrm{abs}}^2 = \overline{\mathrm{N}}_{\mathrm{abs}}\left(1+\frac{\sigma_{\mathrm{p}}^2}{\mathrm{p}^2}\left(\overline{\mathrm{N}}_{\mathrm{abs}}+\eta\overline{\mathrm{p}}\right)\right.$$

Again, if Poisson input with *fixed* mean $\sigma^2_{abs} = \eta N_{inc}(1-\eta) + \eta^2 N_{inc} = \overline{N}_{abs}$, as expected.

Parameters Values:

- QE of LSO powder coating ($81\frac{mg}{cm^2}$) = 0.92.

Stage 1: LSO conversion to visible photons (LSO light yield and intrinsic resolution)

Expression for Variance:

Random Variable N_1, number of visible photons reaching the first image intensifier photocathode. N_1 will be determined by N_{abs} trials of the phosphor yield distribution, with mean output, μ_1, determined by the LSO light yield, and σ_1^2, the variance of that distribution. σ_1^2 is determined by the measured LSO intrinsic resolution, measured in other studies.

Continuing to derive the variance in the same manner, using the law of total variance:

$$\sigma^2_{N1} = E\left[Var\left(N_1 \middle| \widehat{N}_{abs}\right)\right] + Var(E[N_1|N_{abs}]) = \overline{N}_{abs}\sigma_1^2 + Var(\mu_1 N_{abs})$$

$$\sigma^2_{N1} = \overline{N}_{abs}\sigma_1^2 + \mu_1^2\overline{N}_{abs}\left(1 + \frac{\sigma_p^2}{p^2}\left(\overline{N}_{abs} + \eta\overline{p}\right)\right)$$

LSO Parameters:

Reference	Light Yield at 23.5 keV	ΔE/E (FWHM) @ 22 keV
Syntfeld et al.	Not directly stated	~35%
Wanarak et al.	~23000 ph/MeV	~43%

- We will use 40% FWHM, yielding σ1/μ1= 0.17.
- The mean gain from x-ray photon to visible photons is: 23000 ph/MeV, producing 540 photons from one 23.5 keV photon.

Losses from LSO emission to Image Intensifier #1 (II1) photocathode: These losses are due to coupling losses and absorption in the phosphor and in the taper glass. Since these losses are difficult to measure but we roughly know the losses and gains of subsequent stages, we will estimate that the difference between the measured total conversion gain (x-ray photon to counts) and the total gain due to the other stages can be attributed to this loss.

. Gain from other sources*: (540 photons per absorbed x-ray photon) x (4000 photons/photon at II1) x (0.0092 from lens coupling) x (0.25 from Beamsplitters) x (112.9 ADU per incident photon at PIMAX4) = 560887 counts/x-ray photon.

*See subsequent stages for explanation of each total gain figure.

- Measured average total conversion gain = 4300 counts per incident x-ray photon
- QE of LSO (81 mg/cm^2) = 0.92 (XCOM).
- Measured gain = 4670 counts per absorbed x-ray photon
- Losses = 4670/560887 = 0.0082
- Including this in the phosphor-stage gain, the total gain for the conversion from an x-ray to visible photons arriving at the MCP photocathode is μ1= (0.0082) * 540 photons = 4.43 visible photons per x-ray photon

Stage 2: Intensifier Gain at II1 and optical losses to PIMAX camera

Expression for Variance:

- Random Variable: N_2, number of photons reaching PIMAX camera photocathode.
- σ_2^2 is the variance in the II1 output without considering the variance of the input.
- σ_{N2}^2 is the total variance including the variance of the input, N_1

Proceeding in the same manner to find the variance:

$$\sigma_{N2}^2 = E\left[\mathrm{Var}\left(N_2\middle|\widehat{N}_1\right)\right] + \mathrm{Var}(E[N_2|N_1]) = \overline{N}_1\sigma_2^2 + \mathrm{Var}(\mu_2 N_1)$$

$$\sigma_{N2}^2 = \overline{N}_1\sigma_2^2 + +\mu_2^2\left(\overline{N}_{abs}\sigma_1^2 + \mu_1^2\overline{N}_{abs}\left(1 + \frac{\sigma_p^2}{p^2}\left(\overline{N}_{abs} + \eta\overline{p}\right)\right)\right)$$

The mean gain was determined by the manufacturer for this unit to be 4000. We do not have a figure for the noise factor of this image intensifier. However, we can estimate it with known parameters from the device and from other studies.

Parameter Values:

- Lens coupling efficiency = $\left(\frac{M}{2f(1+M)}\right)^2 = 0.00925$, from Gruner et al (2002), for M=0.625, f = 2
- Beamsplitters give another factor of ¼
- Total Gain $\mu_2 = (4000)(0.00925)(0.025) = 9.25$
- Noise from intensifier:
  - Bell et al (1975) suggest the image intensifier noise power factor $\frac{Signal-To-Noise_{OUT}^2}{Signal-to-Noise_{IN}^2}$ cannot be lower than $\frac{1}{QE}$. The S20 photocathode on this MCP has QE=0.13, meaning the noise power factor must be > 8.
  - Vartsky et al. (2009) measured the noise for a similar MCP II from the same company, which also has an S20 photocathode but has higher gain with two MCPs in series and P43 phosphor. They estimate that the photocathode has $\left(\frac{\sigma_{photocathode}}{\mu_{photocathode}}\right)$ of 2.6 (from the 0.13 QE at 420 nm) and they measure the pulse height distribution of the phosphor output (from a single electron excitation) to have $\left(\frac{\sigma_{MCP}}{\mu_{MCP}}\right) =$ 0.68, yielding a total noise power factor of: $\left(1 + (2.6)^2 + \frac{0.68^2}{0.13}\right) = 11.3$ and an effective $\left(\frac{\sigma}{\mu}\right)$ for the

whole intensifier of $\sqrt{(2.6)^2 + \frac{(0.68)^2}{0.13}} = 3.2$. The structure of that intensifier is the same except that it has two MCPs in series. If we assume that the second MCP is not introducing much overall noise (because the electron gain before this stage is so high), we could use a similar noise power factor.

- To be conservative, we will make estimates based on a noise power factor of 10 and 17, or $\left(\frac{\sigma_2}{\mu_2}\right) =$ 3 and 4, respectively (corresponding to a $\left(\frac{\sigma_{MCP}}{\mu_{MCP}}\right)$ of 0.54 and 1.1, respectively).

Stage 3: PIMAX4 ICCDs

Expression for Variance:

- Random Variable: N_3, number of counts (ADU) measured by CCD
- σ_3^2 is the expected variance in the counts without considering the variance of the input
- σ_{N3}^2 is the total variance including the variance of the input, N_2

Proceeding in the same manner to find the variance:

$$\sigma_{N3}^2 = E\left[\mathrm{Var}\left(N_3 \middle| \widehat{N}_2\right)\right] + \mathrm{Var}(E[N_3|N_2]) = \overline{N}_2\sigma_3^2 + \mathrm{Var}(\mu_3 N_2)$$

$$\sigma_{N3}^2 = \overline{N}_2\sigma_3^2 + \mu_3^2\left(\overline{N}_1\sigma_2^2 + \mu_2^2\left(\overline{N}_{abs}\sigma_1^2 + \mu_1^2\overline{N}_{abs}\left(1 + \frac{\sigma_p^2}{p^2}\left(\overline{N}_{abs} + \eta\overline{p}\right)\right)\right)\right)$$

Parameter Values:

- μ_3: $\left(\frac{\mathrm{ADU}}{\text{incident photon}}\right) = (QE)\left(\frac{\mathrm{ADU}}{\text{photoelectron}}\right) = (0.35) * \left(322.6\frac{\mathrm{ADU}}{\text{photoelectron}}\right)$
- Total system gain $\left(322.6\frac{\mathrm{ADU}}{\text{photoelectron}}\right)$ from manufacturer testing certificate.
- $\mu_3 = 112.9\frac{\mathrm{ADU}}{\text{incident photon}}$

Again, the noise of the image intensifier is unknown. However, this intensifier has a much better photocathode, with QE = 0.35 @ ~420nm. The minimum noise figure from this corresponds to 2.85. If there were similar noise in the MCP as we estimated for II1, this would amount to a noise figure between $\left(1 + \left(\frac{\sqrt{0.35(1-0.35)}}{0.35}\right)^2 + \frac{\left(\frac{\sigma_{MCP}}{\mu_{MCP}}\right)^2}{0.35}\right) = 3.68$ and 6.3, for $\left(\frac{\sigma_{MCP}}{\mu_{MCP}}\right)$ of 0.54 and 1.1 again, and an effective $\frac{\sigma_3}{\mu_3}$ for the whole intensifier of 1.6 and 2.3.

DQE Estimate:

Using the variance calculation for the last stage, we can write down the DQE of the detector, with input fluctuations and without.

$$\sigma_{N3}^2 = \overline{N}_2\sigma_3^2 + \mu_3^2\left(\overline{N}_1\sigma_2^2 + \mu_2^2\left(\overline{N}_{abs}\sigma_1^2 + \mu_1^2\overline{N}_{abs}\left(1 + \frac{\sigma_p^2}{p^2}\left(\overline{N}_{abs} + \eta\overline{p}\right)\right)\right)\right)$$

$$\sigma_{N3}^2 = \overline{N}_{abs}\mu_1\mu_2\sigma_3^2 + \mu_3^2\overline{N}_{abs}\mu_1\sigma_2^2 + \mu_3^2\mu_2^2\overline{N}_{abs}\sigma_1^2 + \mu_3^2\mu_2^2\mu_1^2\overline{N}_{abs}\left(1 + \frac{\sigma_p^2}{p^2}\left(\overline{N}_{abs} + \eta\overline{p}\right)\right)$$

$$\mu_{N3} = \overline{N}_{abs}\mu_1\mu_2\mu_3$$

$$\text{(Measured Signal-to-Noise)}^2 = \frac{\mu_{N3}^2}{\sigma_{N3}^2}$$

$$\frac{\mu_{N3}^2}{\sigma_{N3}^2} = \frac{\left(\overline{N}_{abs}\mu_1\mu_2\mu_3\right)^2}{\overline{N}_{abs}\mu_1\mu_2\sigma_3^2 + \mu_3^2\overline{N}_{abs}\mu_1\sigma_2^2 + \mu_3^2\mu_2^2\overline{N}_{abs}\sigma_1^2 + \mu_3^2\mu_2^2\mu_1^2\overline{N}_{abs}\left(1 + \frac{\sigma_p^2}{p^2}\left(\overline{N}_{abs} + \eta\overline{p}\right)\right)}$$

$$\frac{\mu_{N3}^2}{\sigma_{N3}^2} = \frac{\overline{N}_{abs}}{1 + \frac{1}{\mu_1\mu_2}\frac{\sigma_3^2}{\mu_3^2} + \frac{1}{\mu_1}\frac{\sigma_2^2}{\mu_2^2} + \frac{\sigma_1^2}{\mu_1^2} + \frac{\sigma_p^2}{p^2}\left(\overline{N}_{abs} + \eta\overline{p}\right)}$$

$$\text{(Ideal signal-to-noise)}^2 = \overline{N}_{inc}$$

$$\text{DQE} = \frac{(\text{Signal}-\text{to}-\text{Noise})^2}{(\text{Ideal Signal}-\text{to}-\text{Noise})^2} = \frac{\overline{N}_{abs}}{\overline{N}_{inc}\left(1 + \frac{1}{\mu_1\mu_2\mu_3^2}\frac{\sigma_3^2}{} + \frac{1}{\mu_1\mu_2^2}\frac{\sigma_2^2}{} + \frac{\sigma_1^2}{\mu_1^2} + \frac{\sigma_p^2}{p^2}\left(\overline{N}_{abs} + \eta\overline{p}\right)\right)}$$

$$\text{Measured DQE} = \frac{\eta}{1 + \left(\frac{1}{\mu_1\mu_2}\right)\frac{\sigma_3^2}{\mu_3^2} + \left(\frac{1}{\mu_1}\right)\frac{\sigma_2^2}{\mu_2^2} + \frac{\sigma_1^2}{\mu_1^2} + \frac{\sigma_p^2}{p^2}\left(\overline{N}_{abs} + \eta\overline{p}\right)}$$

Estimated DQE of system ($\sigma_p^2 = 0$) using previously defined parameters:

$\eta = 0.92$, $\mu_1 = 4.43$, $\frac{\sigma_1}{\mu_1} = 0.17$, $\mu_2 = 9.25$, $\left(\frac{\sigma_2}{\mu_2}\right) = 3$ or 4, $\left(\frac{\sigma_3}{\mu_3}\right) = 1.6$ and 2.3.

High Estimate (assuming better MCP performance):

$$\frac{0.92}{1 + \frac{1}{(4.43)(9.25)}1.6^2 + \frac{1}{4.43}3^2 + 0.17^2} = 0.295$$

Low Estimate (assuming worse MCP performance):

$$\frac{0.92}{1+\frac{1}{(4.43)(9.25)}2.3^2+\frac{1}{4.43}4^2+0.17^2}=0.193$$

References:

Bell, R. L. (1975). Noise Figure of the MCP Image Intensifier Tube. IEEE Transactions on Electron Devices, 22(10), 821–829. https://doi.org/10.1109/T-ED.1975.18229

Berger, M., Hubbell, J., Seltzer, S., Chang, J., Coursey, J., Sukumar, R., Zucker, D. & Olsen, K., (2010). XCOM: Photon Cross Section Database (version 1.5). http://physics.nist.gov/xcom

Ciamberlini, C., Longobardi, G., Ramazza, P. L., Residori, S. (1994). New approach to noise factor measurement of imaging devices. Optical Engineering, 33(3), 845. https://doi.org/10.1117/12.157680

Gruner, S. M., Tate, M. W., Eikenberry, E. F. (2002). Charge-coupled device area x-ray detectors. Review of Scientific Instruments, 73(8), 2815. https://doi.org/10.1063/1.1488674

Syntfeld-Kazuch, A., Moszyński, M., Świderski, Ł., Szczęśniak, T., Nassalski, A., Melcher, C. L., … Nowaczyk, M. (2009). Energy resolution of calcium co-doped LSO:Ce scintillators. *IEEE Transactions on Nuclear Science*, *56*(5), 2972–2978. https://doi.org/10.1109/TNS.2009.2028235

Vartsky, D., Feldman, G., Mor, I., Goldberg, B., Bar, D., Dangendorf, V. (2009). Signal and noise analysis in TRION - Time-Resolved Integrative Optical Fast Neutron detector. Journal of Instrumentation, 4(2). https://doi.org/10.1088/1748-0221/4/02/P02001

Wanarak, C., Chewpraditkul, W., Phunpueok, A. (2012). Light yield non-proportionality and energy resolution of Lu 1.95Y0.05SiO5:Ce and Lu2SiO 5:Ce scintillation crystals. Procedia Engineering, 32, 765–771. https://doi.org/10.1016/j.proeng.2012.02.010